Final Report

Wayne Lin[1]

[1]Affiliation not available

December 02, 2025

Abstract

This work reports the design, fabrication, and characterization of a silicon photonic chip containing two Mach–Zehnder interferometers and a ring resonator. A compact waveguide model informs analytical transfer-function calculations and layout design. Fabricated using 100 keV electron-beam lithography, the devices show measured spectra consistent with simulations after baseline removal. Group-index extraction confirms MZI agreement with corner analysis, while the ring resonator exhibits higher sensitivity to fabrication variations.

1 Introduction

Silicon photonics is growing as a practical way to build compact and low-cost optical circuits. In this project, I look at two basic building blocks: the Mach–Zehnder interferometer (MZI), used for modulation and filtering, and the ring resonator, useful for wavelength selection and sensing. [(Chrostowski and Hochberg, 2015)] Both are simple but powerful examples of how integrated photonics can work in real systems.

2 Theory

2.1 Waveguide Compact Model

The effective index expansion:

$$n_{\text{eff}}(\lambda) \approx a_1 + a_2(\lambda - \lambda_0) + a_3(\lambda - \lambda_0)^2. \tag{1}$$

Group index:

$$n_g = n_{\text{eff}} - \lambda \frac{dn_{\text{eff}}}{d\lambda}. \tag{2}$$

2.2 Y-Branch

An ideal Y-branch splits power equally (-3 dB per port). Interference depends on phase:

$$P_{\text{out}} \propto |E_1 \pm E_2|^2. \tag{3}$$

2.3 Mach–Zehnder Interferometer

Normalized transfer function:

$$T_{\text{MZI}}(\lambda) = \frac{1}{2}\left[1 + \cos(\Delta\phi(\lambda))\right], \tag{4}$$

where

$$\Delta\phi(\lambda) = \frac{2\pi}{\lambda} n_g \Delta L. \tag{5}$$

Free spectral range:

$$\Delta\lambda_{\mathrm{FSR}} = \frac{\lambda^2}{n_g\,\Delta L}. \tag{6}$$

2.4 Ring Resonator

All-pass transfer function:

$$T_{\mathrm{ring}}(\lambda) = \left| \frac{t - Ae^{-i\phi}}{1 - tAe^{-i\phi}} \right|^2, \tag{7}$$

with t the amplitude transmission of the coupler, $A = e^{-\alpha L/2}$ round-trip loss, and $\phi = \beta L$. Resonance condition:

$$m\lambda = n_{\mathrm{eff}} L. \tag{8}$$

Free spectral range:

$$\Delta\lambda_{\mathrm{FSR}} = \frac{\lambda^2}{n_g L}. \tag{9}$$

3 Chip Design and Simulation Results

3.1 Waveguide Compact Model Simulation

A compact model simulation was conducted in Lumerical MODE module. The waveguide material is Si and the cladding material is SiO_2. Lumerical's built-in dispersion data was used for the simulations.

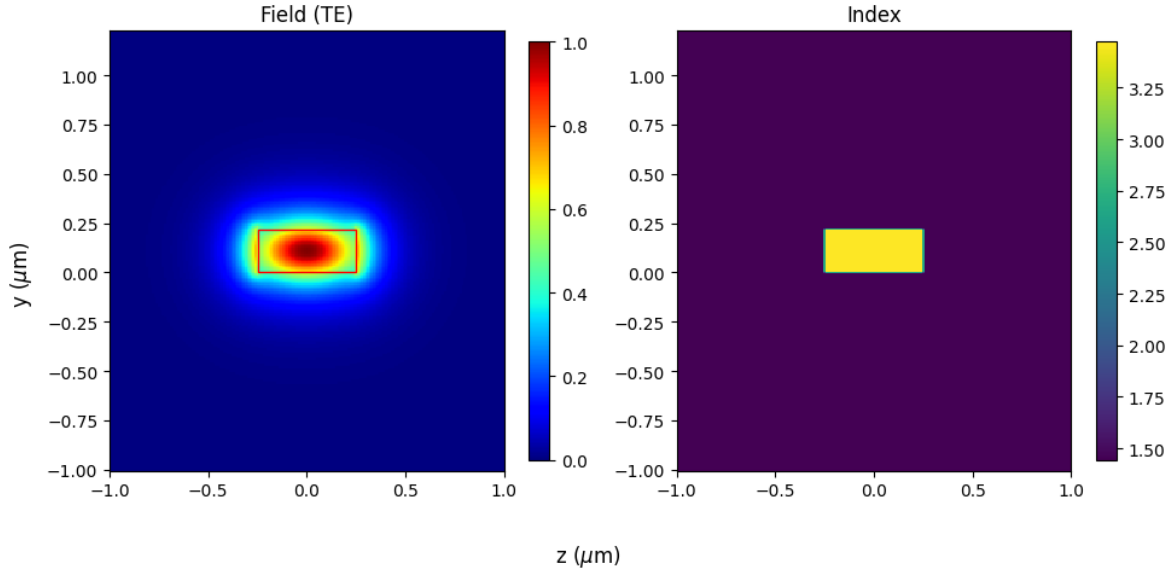

Figure 1: Waveguide Compact Model Simulation

3.2 MZI & Ring Resonator Model Calculation

From the n_{eff} and n_g values obtained from the compacr model simulation result. One can calculate the transmission spectrum of each component. The design values are listed in the table below.

Component	Parameter	Value
MZI1	ΔL	300 μm
MZI2	ΔL	163.43 μm

Component	Parameter	Value
Ring	R	10 µm

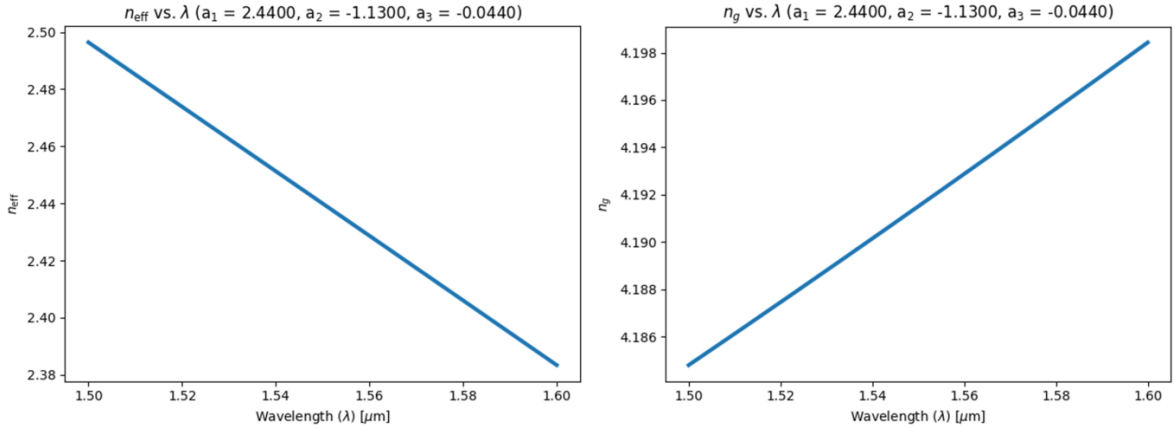

Figure 2: Effective Index and Group Index

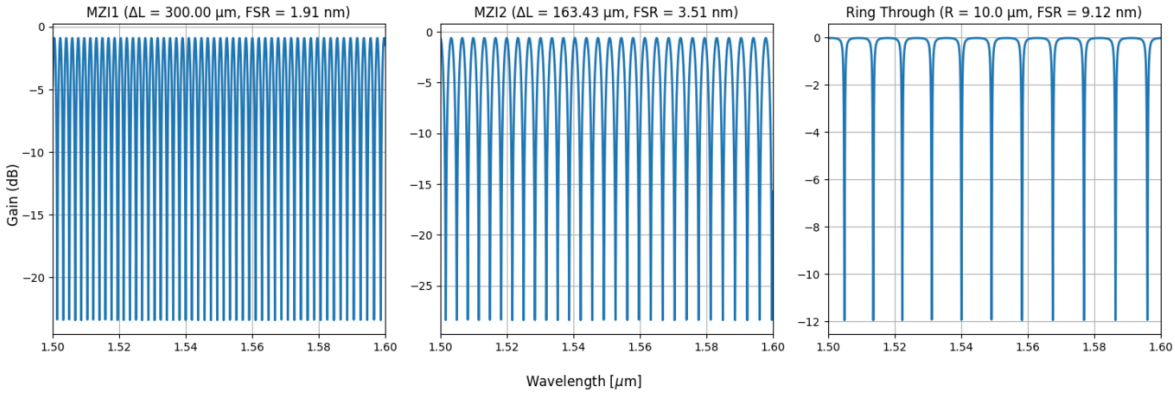

Figure 3: MZI Transfer Functions and Ring Through Transmission

3.3 Chip Design and Layout

The designs layout was created by klayout according to the specification of the foundry. A baseline circuit was included for filtering out the effect introduced by grating couplers.

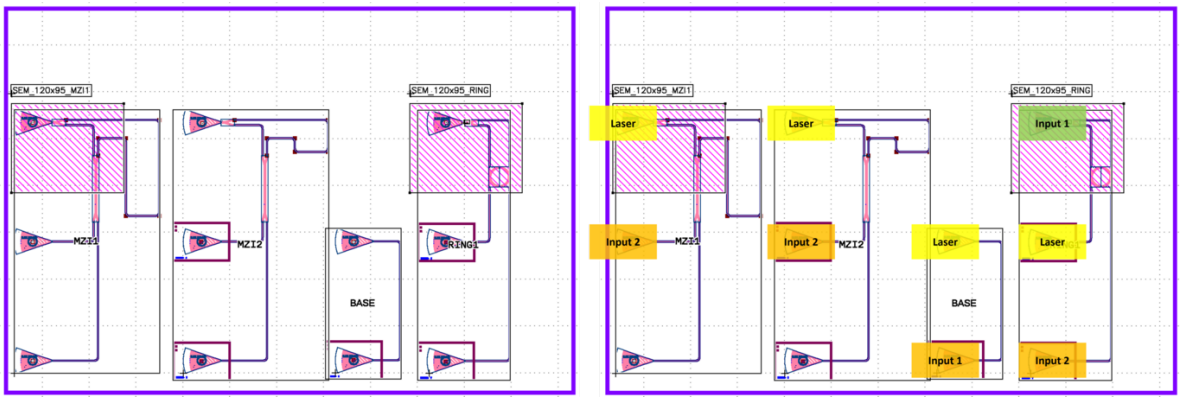

Figure 4: Final layout for chip fabrication (left) and the corresponding layout annotated with port labels for circuit-simulation data collection (right).

3.4 Preliminary Simulation Results

The simulation result by Lumerical Interconnect module showed the basline curves in all collected spectra, and it was removed by the substraction of baseline spectrum.

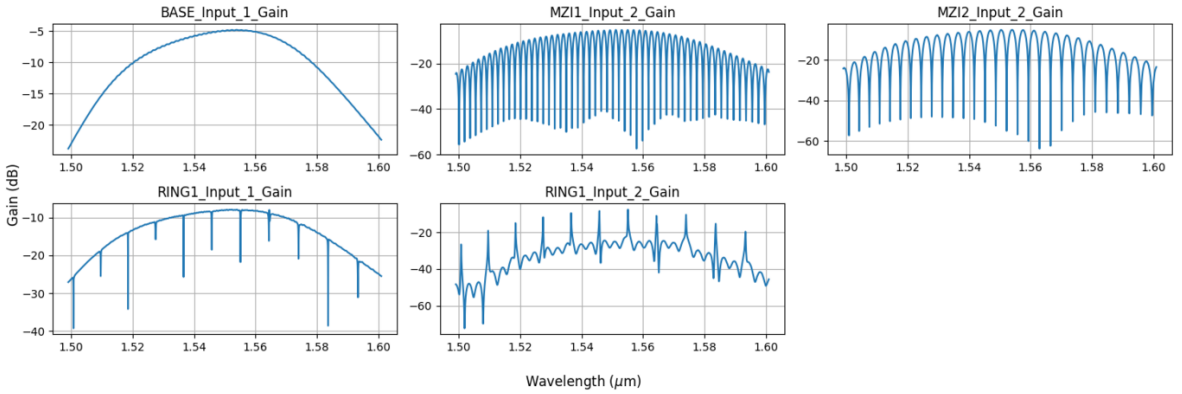

Figure 5: Simulation Results by Lumerical Interconnec

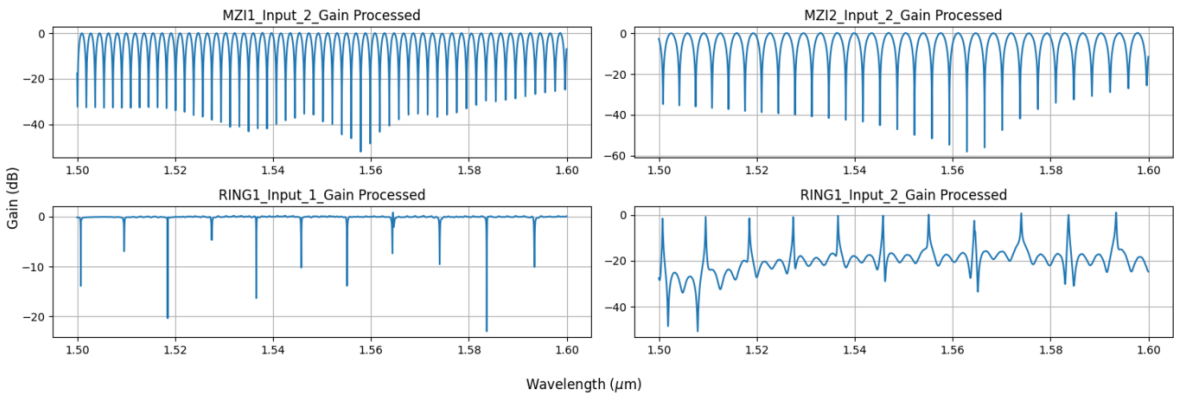

Figure 6: Simulation Result after Baseline Removal

The comparison of simulated MZI spectrum with model calculation showed generally good agreement

despite minor phase shift. For ring resonator the phase shift is more prominent, but the pitch is consistent to model calculation.

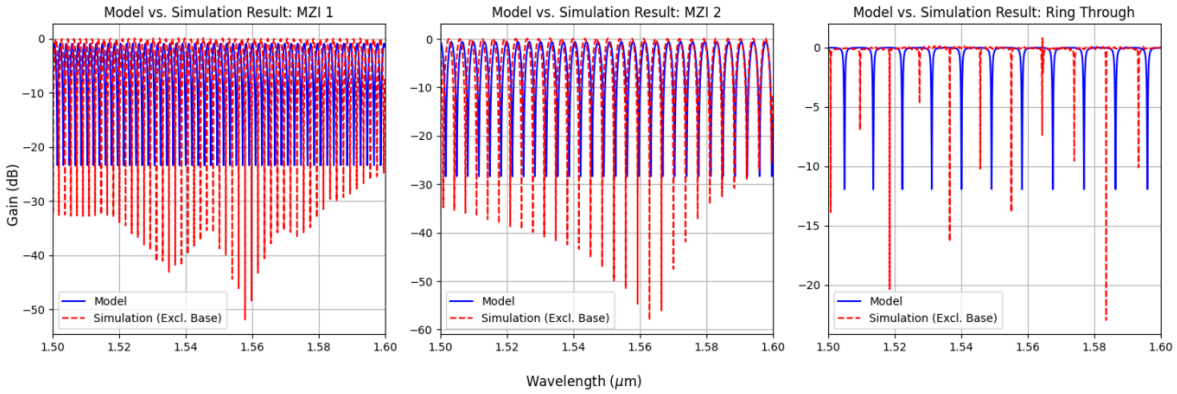

Figure 7: Model Calculation vs. Simulation Results

4 Fabrication

Two chips were fabricated in this course. Either report on one dataset, or on both. Choose the text as appropriate.

4.1 Washington Nanofabrication Facility (WNF) silicon photonics process:

The devices were fabricated using 100 keV Electron Beam Lithography [(Bojko et al., 2011)]. The fabrication used silicon-on-insulator wafer with 220 nm thick silicon on 3 μm thick silicon dioxide. The substrates were 25 mm squares diced from 150 mm wafers. After a solvent rinse and hot-plate dehydration bake, hydrogen silsesquioxane resist (HSQ, Dow-Corning XP-1541-006) was spin-coated at 4000 rpm, then hotplate baked at 80 °C for 4 minutes. Electron beam lithography was performed using a JEOL JBX-6300FS system operated at 100 keV energy, 8 nA beam current, and 500 μm exposure field size. The machine grid used for shape placement was 1 nm, while the beam stepping grid, the spacing between dwell points during the shape writing, was 6 nm. An exposure dose of 2800 μC/cm2 was used. The resist was developed by immersion in 25% tetramethylammonium hydroxide for 4 minutes, followed by a flowing deionized water rinse for 60 s, an isopropanol rinse for 10 s, and then blown dry with nitrogen. The silicon was removed from unexposed areas using inductively coupled plasma etching in an Oxford Plasmalab System 100, with a chlorine gas flow of 20 sccm, pressure of 12 mT, ICP power of 800 W, bias power of 40 W, and a platen temperature of 20 °C, resulting in a bias voltage of 185 V. During etching, chips were mounted on a 100 mm silicon carrier wafer using perfluoropolyether vacuum oil.

5 Experimental Data

5.1 Data Acquisition Locations & SEM Images

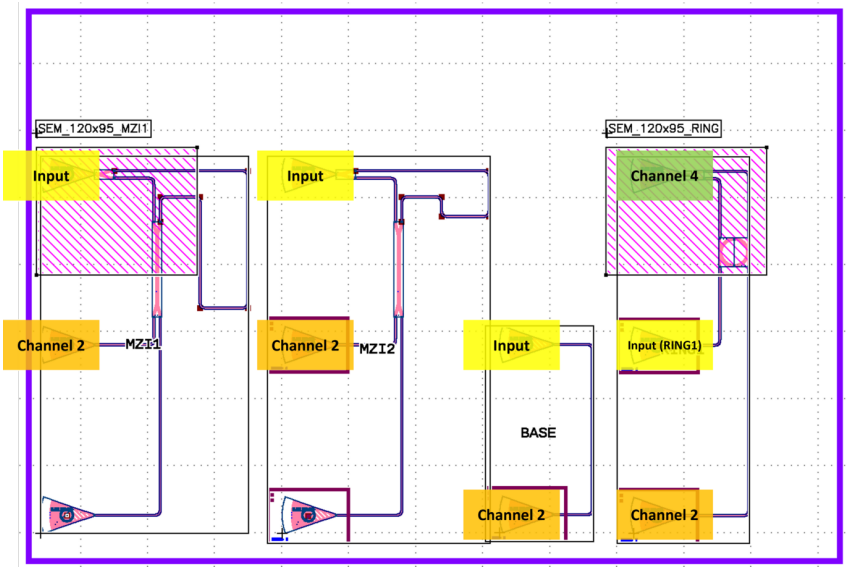

Figure 8: Layout with annotated data collection locations, including measurment port location and SEM image locations

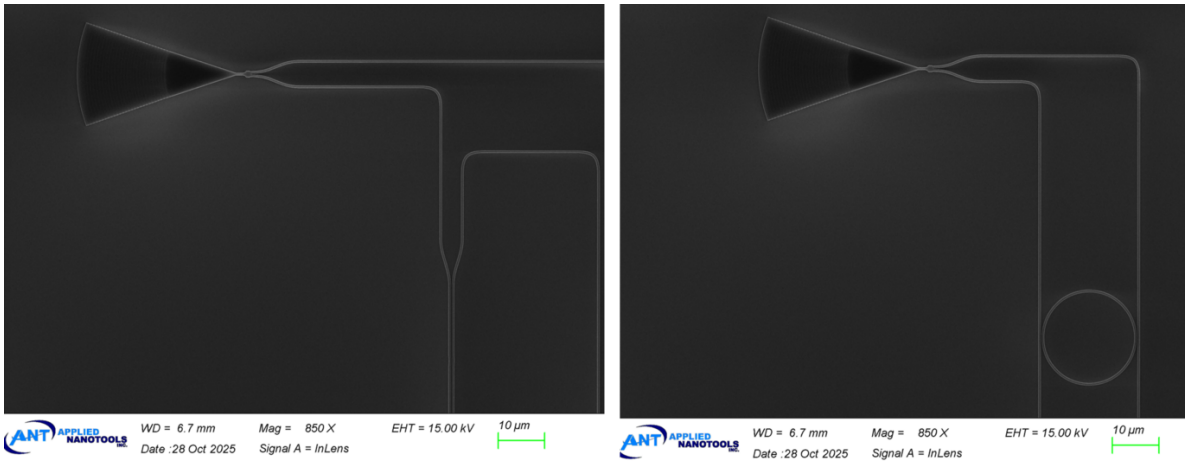

Figure 9: SEM images of the MZI1 device (left) and the ring resonator (right) in the fabricated photonic chip.

5.2 Measurement Results

The measurement result showed good agreement with simulation result. Phase shift still persists in the result of ring resnator.

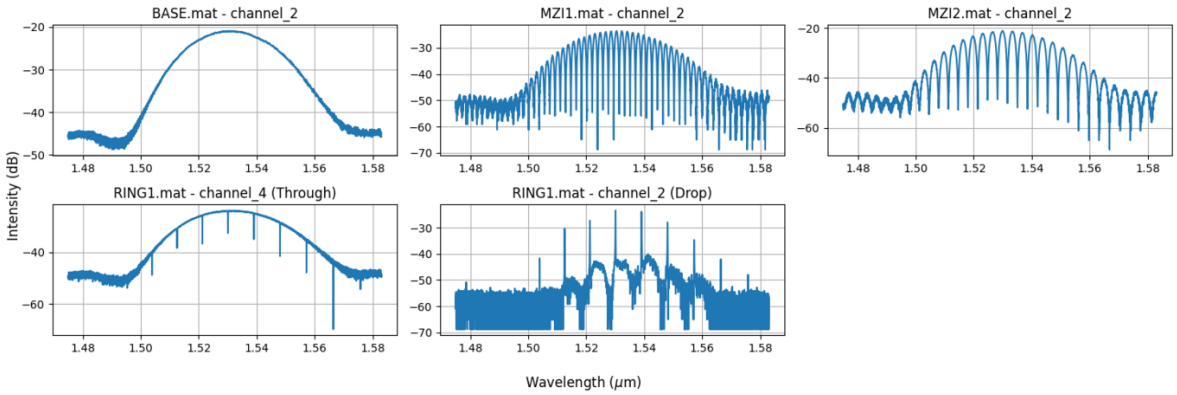

Figure 10: Measured spectrum of fabricated photonic chip

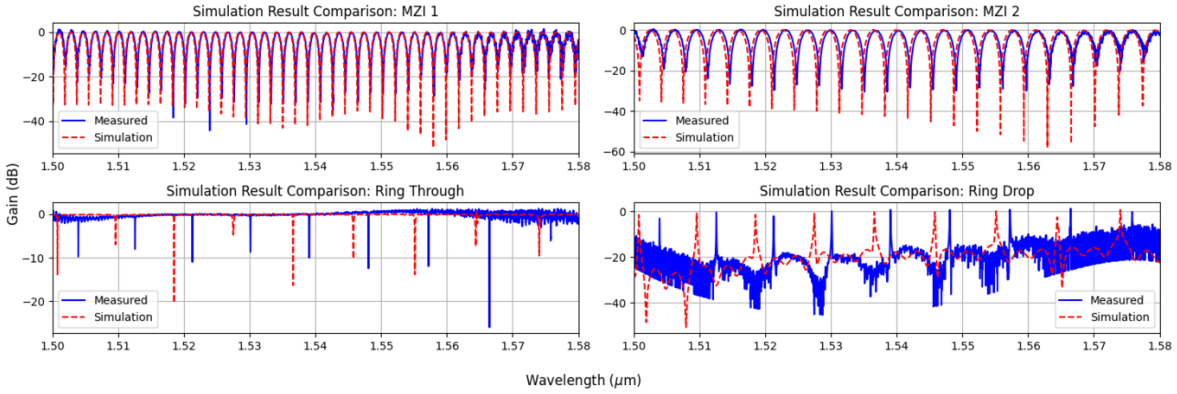

Figure 11: Measured and simulated spectral responses for MZI1, MZI2, the ring through port, and the ring drop port. The measured spectra are shown with the baseline excluded for clarity.

6 Analysis

6.1 MZI Transfer Function Fitting

With autocorrelation and MZI transfer function fitting on the measurement data. We can obtain the group index and effective index of the waveguide.

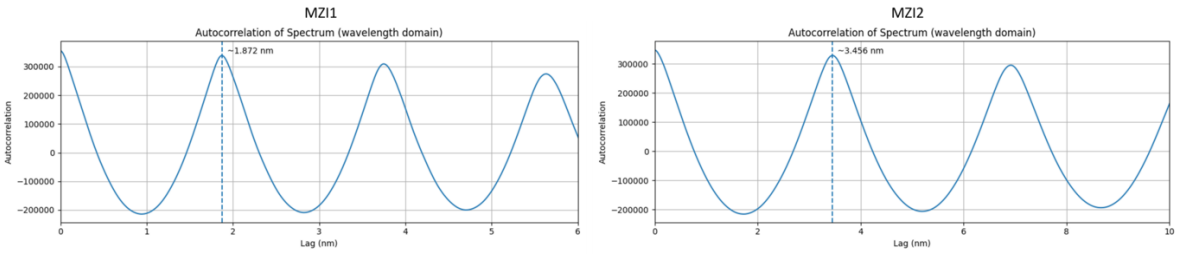

Figure 12: FSR calculation using spectrum autocorrelation on MZI1 and MZI2 spectrum

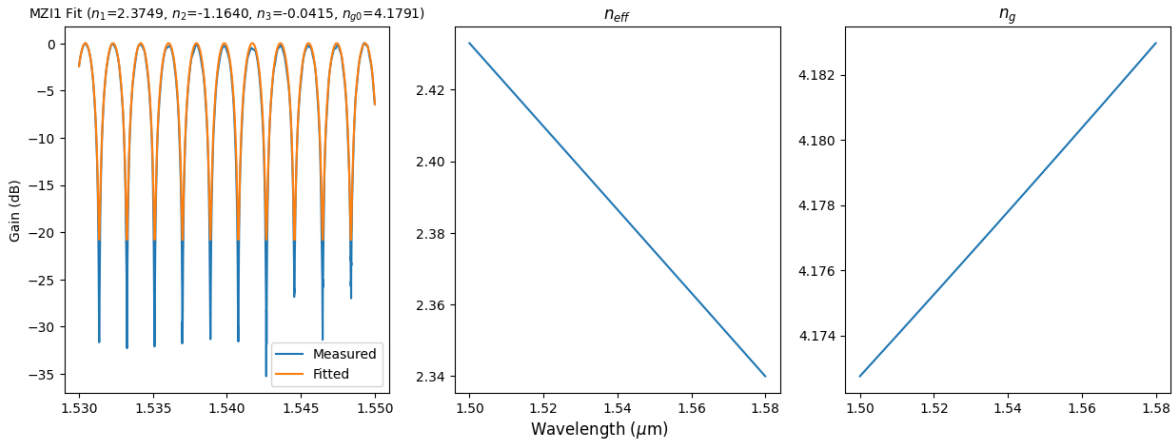

Figure 13: Fitted MZI1 transfer function and the exctracted n_{eff} and n_g versus wavelength.

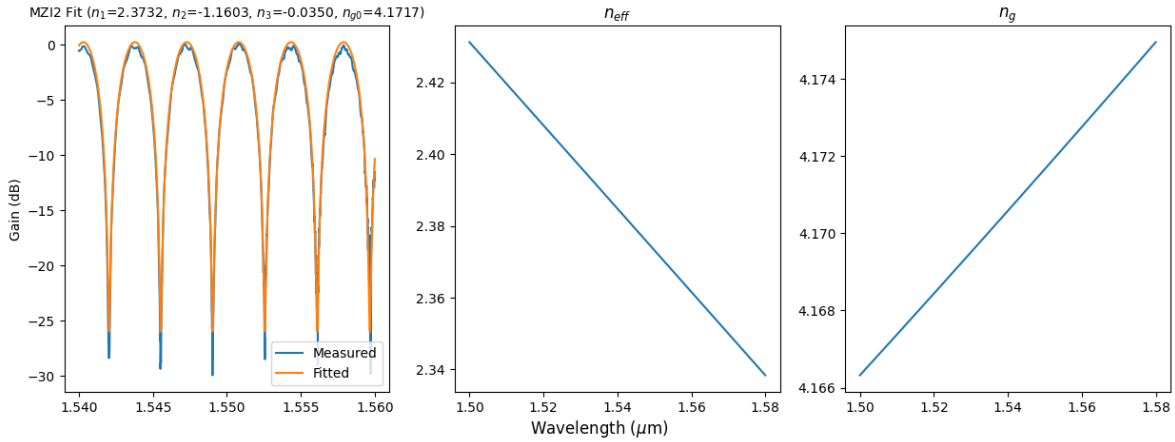

Figure 14: Fitted MZI2 transfer function and the exctracted n_{eff} and n_g versus wavelength.

6.2 Ring FSR

The FSR of ring resonator can be extracted by peak location, and the group index relation can be extracted via fitting.

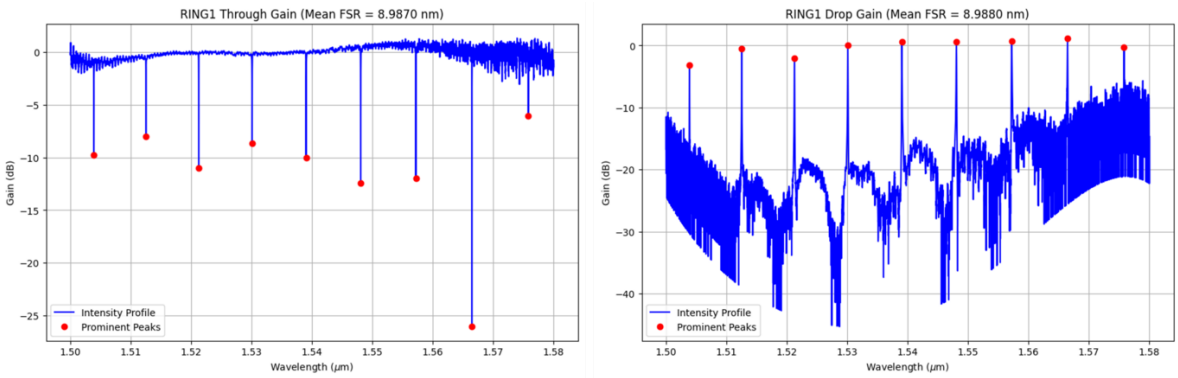

Figure 15: Mean FSR extracted from the through and drop spectra of the ring resonator.

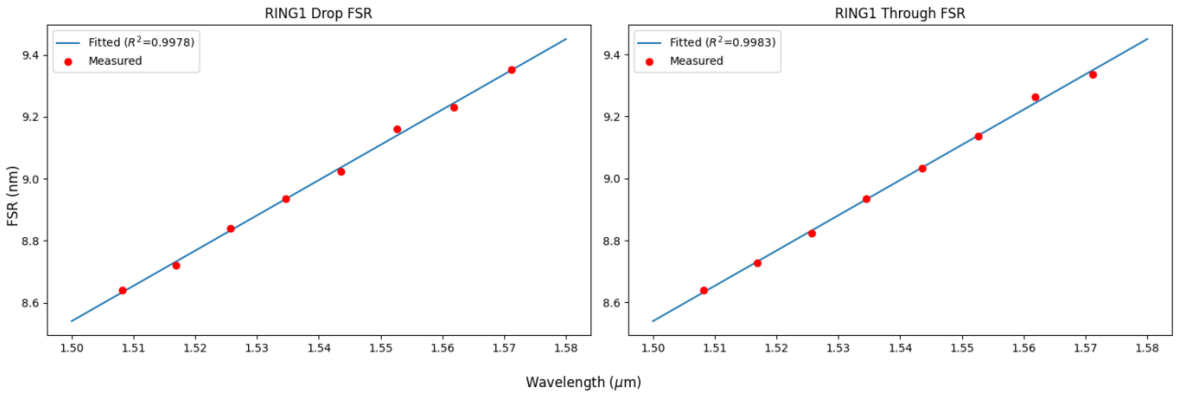

Figure 16: Fitted FSR–wavelength trends for the ring resonator (drop and through ports).

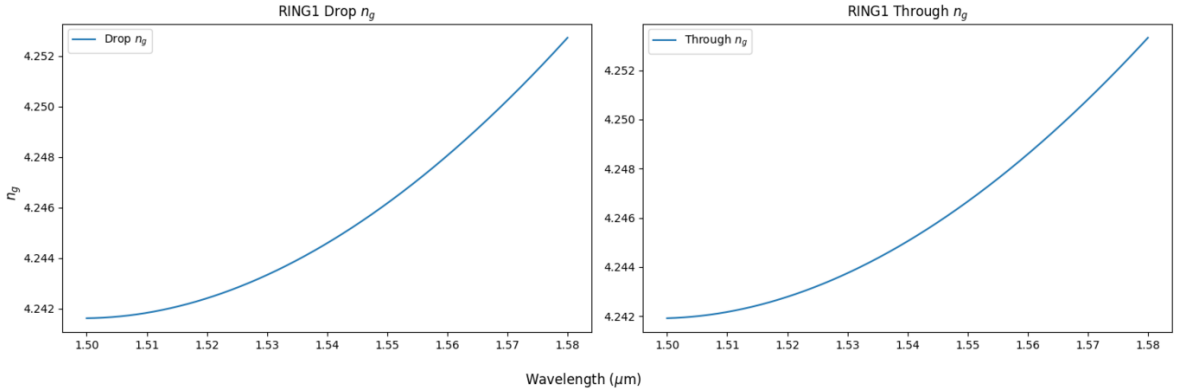

Figure 17: Fitted n_g for ring resonator (drop and through ports).

6.3 Corner Analysis

By varying different waveguide dimensions within the process window of the foundry, we can obtained a map for the possible group index and use it to estimate the actual waveguide dimension in the fabrication.

Component	n_g
MZI1	4.1791
MZI2	4.1717
Ring (Drop)	4.2461
Ring (Through)	4.2467

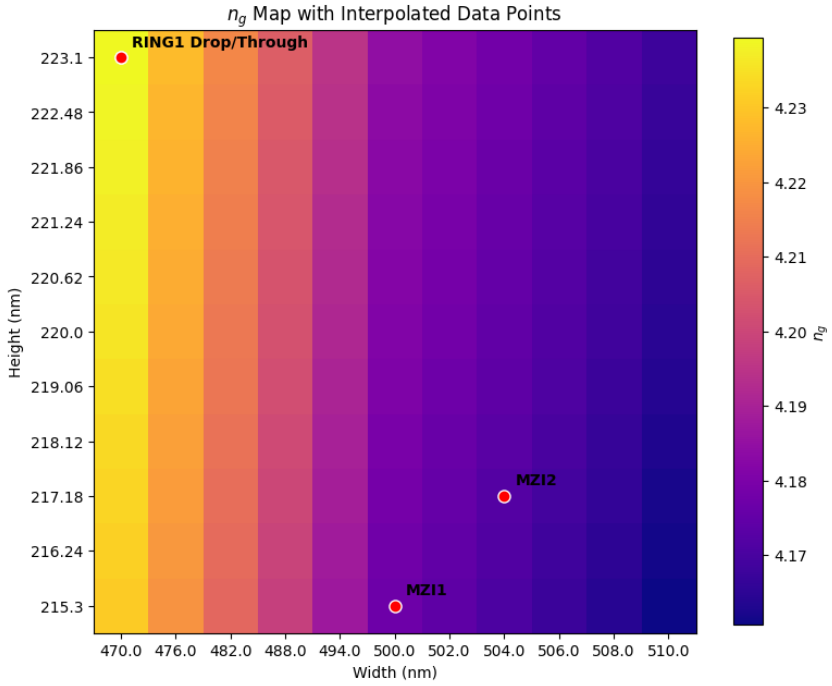

Figure 18: Simulated n_g map with measured/interpolated n_g values plotted for MZI1, MZI2, and the ring resonator.

7 Conclusion

The measurement results show generally good agreement with simulation. Showcasing a valid design package provided by course. The n_g extracted by ring resonator is outside of the corner analysis, indicating that the component is more sensitive to process.

8 Acknowledgements

I/We acknowledge the edX UBCx Phot1x Silicon Photonics Design, Fabrication and Data Analysis course, which is supported by the Natural Sciences and Engineering Research Council of Canada (NSERC) Silicon Electronic-Photonic Integrated Circuits (SiEPIC) Program. The devices were fabricated by Richard Bojko at the University of Washington Washington Nanofabrication Facility, part of the National Science Foundation's National Nanotechnology Infrastructure Network (NNIN), and Cameron Horvath at Applied Nanotools, Inc. Enxiao Luan performed the measurements at The University of British Columbia. We acknowledge Lumerical Solutions, Inc., Mathworks, Mentor Graphics, Python, and KLayout for the design software.

References

Richard J. Bojko, Jing Li, Li He, Tom Baehr-Jones, Michael Hochberg, and Yukinori Aida. Electron beam lithography writing strategies for low loss high confinement silicon optical waveguides. *Journal of Vacuum Science & Technology B: Microelectronics and Nanometer Structures*, 29(6):06F309, 2011. doi: 10.1116/1.3653266. URL http://dx.doi.org/10.1116/1.3653266.

Lukas Chrostowski and Michael Hochberg. *Silicon Photonics Design*. Cambridge University Press (CUP), 2015. doi: 10.1017/cbo9781316084168. URL http://dx.doi.org/10.1017/cbo9781316084168.